Proceedings World Geothermal Congress 2000
Kyushu - Tohoku, Japan, May 28 - June 10, 2000

2-D INVERSION OF DC RESISTIVITY DATA FROM THE CERRO PRIETO GEOTHERMAL AREA, MEXICO

Adolfo S. Charré-Meza, Marco A. Pérez-Flores and **Enrique Gómez-Treviño**
Earth Sciences Division, CICESE, km 107 Carr. Tijuana-Ensenada, Ensenada, B.C., México.

Keywords: Cerro Prieto, Mexico, resistivity, inversion.

ABSTRACT

The Cerro Prieto Geothermal area, one of several geothermal areas in Mexico, was the first to be developed and, at the present, it is the largest in the country (620 MW). Because of its importance, many geophysical, geochemical and geohydrological techniques have been applied in order to have a better understanding of the spatial distribution of the reservoir. From the geophysical point of view, DC resistivity and Magnetotelluric methods have demonstrated to be very successful in resolving the spatial distribution of conductivity in the subsurface. With this purpose, several field works have been conducted to collect DC resistivity data. In this way, the Mexican Commission of Electricity (CFE) collected in 1977-79 more than 411 deep Schlumberger soundings (maximum *AB/2= 5 km*), arranged in lines. These give us the opportunity to attempt a two-dimensional inversion of such lines. Also, in 1977-79 the Lawrence Berkeley Laboratory collected three long-offset dipolo-dipole lines in the same region (maximum *n= 8; a=1 km*). We are inverting Schlumberger and dipole-dipole data jointly, where possible, or just Schlumberger data. This give us a picture of the main features of the principal reservoir of the Cerro Prieto Geothermal area. This new information is compared with different information available of the whole geothermal area.

1. INTRODUCTION.

Resistivity methods in geophysics have been very successful in Geothermal exploration. Normally, high temperatures in a permeable environment lower the electrical resistivity, so the resistivity method finds conductive spots that normally correspond to possible reservoir locations (e.g., Pérez-Flores and Gómez-Treviño, 1997).

There are several inversion techniques in DC resistivity methods. The fastest are such that work with the approximation for low resistivity contrast. Such techniques are called *imaging,* and the resulting inversions (resistivity sections) are named *resistivity images*. We use a non-linear integral equation (Gómez-Treviño, 1987), and after the approximation for low resistivity contrast we get a linear integral equation that can easily be used for inversion, with the advantage that we do not need to specify an initial model like conventional *imaging* techniques (Cavazos-Garza and Gómez-Treviño, 1989; Li and Oldenburg, 1992). Our method is used to interpret the resistivity data from the Cerro Prieto Geothermal area. A very big campaign of collecting data was carried on between 1977 and 1979. The interpretation of such data gave us a lot of information about the hydrological model , the influence of the Cucapá Sierra, the granitic basement, and the possible influence of the buried Cerro Prieto Fault.

2.- METHOD DESCRIPTION

The resistivity inversion method is based on an integral equation that relates the zero frequency electric field measured on surface and the electrical resistivity in the subsurface, through a weighting function that depends of the electric field in the subsurface and the electrical Green function of the whole heterogeneous half-space (Gómez-Treviño, 1987). For a point source located at *A* and a point receiver located at *M*,

$$\mathbf{E}(\mathbf{r_A},\mathbf{r_M}) = -\int \mathbf{G}(\mathbf{r_M},\mathbf{r'},\rho)\bullet\mathbf{E}(\mathbf{r'},\mathbf{r_A},\rho)\frac{dv'}{\rho(\mathbf{r'})} \quad . \tag{1}$$

Equation (1) is different from the classical scattering equation (Hohmann, 1975), because here we relate directly the observation with the electrical property of the Earth and not thought perturbations of the later. Equation (1) is very useful when we assume the weighting function to be that of a homogeneous half-space. This approximation is valid not only for low resistivity contrasts in the subsurface, but also for moderate contrast. From equation (1) we can arrive to equation (2) bellow, (see Pérez-Flores, 1995). For a typical electrical array of a source dipole (*A,B*) and a receiver dipole (*M,N*), along the *x* coordinate and over a 2-D heterogeneous half-space, we have,

$$\log \rho_a(x_A, x_B, x_M, x_N) = \frac{[g]^{-1}}{\pi}\int_0^{\infty}\int_{-\infty}^{\infty} M(x_A, x_B, x_M, x_N)\log\rho(x', z') \tag{2}$$

where *g* is the geometric factor. Equation (2) is valid for any collinear tetraelectrode array: Dipole-dipole, Schlumberger or Wenner. Equation (2) has the advantage that relates directly the measured apparent resistivity with the heterogeneous half-space resistivity throughout a weighting function that depends only on the electrodes position and it is independent of any constant resistivity, as in Cavazos-Garza and Gómez-Treviño, 1989 or Li and Oldenburg (1992). Equation (2) is a linear integral equation that can be used in inversion in order to get the subsurface resistivity distribution. In general,

$$M(x_A,x_B,x_M,x_N) = N(x_A,x_M) - N(x_A,x_N) - N(x_B,x_M) + N(x_B,x_N) \tag{3}$$

For a 2-D resistivity distribution, we assume that resistivity does not vary perpendicular to the prospecting line (*y* coordinate). In this case,

$$N(x_i,x_j) = \int_{-\infty}^{\infty} \frac{(x'-x_i)(x_j-x') - y'^2 - z'^2}{\left[(x'-x_i)^2 + y'^2 + z'^2\right]^{3/2}\left[(x_j-x')^2 + y'^2 + z'^2\right]^{3/2}}\, dy' \tag{4}$$

Equation (4) can be solved numerically, but also has a complex analytical solution in terms of elliptic integrals (Pérez-Flores, 1995).
Equation (2) can be posed as a linear system of equations

$$\mathbf{Y}=\mathbf{AX}\ , \tag{5}$$

where

$$\mathbf{Y}=\log\rho_a\ ,\quad \mathbf{X}=\log\rho\ ,\quad \mathbf{A}=\text{Discretized integrand} \tag{6}$$

We assume that the half-space consists of a set of small 2-D prisms with a constant resistivity in every one. We solve equation (5) by means of quadratic programming, minimizing the quadratic norm of residual plus the first spatial derivatives of the resistivity distribution. In this way, we get the best combination of prism resistivities (ρ_i), whose response, best fit the data and also give us the flattest models.

$$F(\rho_i)=\left\|\mathbf{Y}-\mathbf{AX}\right\|^2+\beta\left\|\mathbf{DX}\right\|^2 \tag{7}$$

This objective function also takes into consideration the observation error through a covariance error matrix, in order to not fit beyond the expected data error. The factor β is determined empirically and as it increases, the model gets flatter. In a normal PC computer it is very fast to run a model. 93% is expended in getting the matrix **A** and 7% in getting a model, so it is very easy and fast to get many different models by changing β value, and keeping the most coherent model.

3.- APPLICATION TO THE GEOTHERMAL AREA

Cerro Prieto Geothermal field is located at the Northwest of Mexico, close to the border with U.S.A. (Figure 1). This geothermal area is located in the contact between the Pacific and Northamerica Plates. This border is part of the San Andreas Fault system that crosses the Baja California peninsula close to the Colorado River output and sinks into the Baja California Gulf. This fault is responsible for the peninsula separation from the Mexican main land between 12 and 6 m.y. ago. In the separation, a large basin was formed (the Gulf). Despite the main lateral faulting, there also exist perpendicular components of the echelon type. There are dispersive points where new crust is emerging. Submarine fumaroles have been seen in the Gulf where such dispersive points can be located. It is possible that Cerro Prieto area is over a dispersive point in land, where a characteristic pull-apart-basic was formed, but now this has been filled from the north by alluvial sediments of the Colorado river, from the west the Hardy River, and from the south the salty floods of the Gulf.
Presently, the exploitation area is over a sedimentary basin with a depth of around 4000 m, flanked to the west by the Cucapá Sierra and to the east by a broad area of alluvial sediments from Colorado river. Production in the area began by making some exploratory and production holes on the west of the railroad and now has expanded to the east. Between 1977-79 an extensive campaign was carried out to obtain Dipole-dipole and Schlumberger data. The Lawrence Berkeley Laboratory collected two dipole-dipole lines to the north of the present production zone, the Mexican Commission of Electricity (CFE) collected more than 400 Schlumberger soundings over a very wide area (Wilt, *et al*., 1978; Figure 1). Most of these soundings were arranged in Schlumberger lines with SW-NE main direction. The purpose of this work is to interpret such dipole-dipole lines individually and jointly with the their closest Schlumberger line. Also, we interpret the most important 20 Schlumberger lines in order to define the conductive structure below the surface of the Cerro Prieto area. All these interpretations are based on the technique described before with the idea of getting better results and extract new geological and hydrological information of the geothermal area.

4.- RESISTIVITY IMAGES

Figure 2 shows a resistivity image obtained by the inversion of one dipole-dipole line jointly with its closest Schlumberger line. We got more features of the conductive structure by using joint inversion as opposed to individual inversions.
Resistivity image from Figure 2 began 5 km from the Cucapá Sierra and runs along 23 km over the Cerro Prieto basin, and 3 km to the north from the production zone (Figure 1).
We see in Figure 2 a resistive basement on the west side that can correspond to the influence of the granitic rocks and clastic sediments of the Cucapá Sierra. From kilometer 1 to 20 extends the main conductive area under the geothermal zone. This area corresponds to permeable quaternary sands with interdigitized clays where the reservoir is located. High temperatures are found all around this area, but the present production zone is located below kilometers 8 to 9, at a depth of 1.5 km. Gravity data suggest that granitic basement must be located below 3.0 km depth, so our resistivity image agrees with the gravity model proposed (Gupta and Ramani, 1980). From kilometer 14 to 23 begins a shallow resistive layer that corresponds to the intrusion of fresh water from the Colorado river, whose resistivity must be close to 80 ohms-m.
In Figure 3 is shown the resistivity image obtained from the Schlumberger line 6. This line is the closest to the present production zone. The east side of the line is further from the Cucapá Sierra however a resistive feature is shown, because of the granitic clastic sediments. From kilometer 0 to 12 also is shown the permeable sands unit where the reservoir is located. Normally, the rule says that as temperature increases, the resistivity decreases. However, in Cerro Prieto this is not always true, because the present reservoir (between kilometer 3 and 5.5) has a resistivity of 4 to 6 ohm-m with temperatures higher than 300 °C while the sands have a resistivity of 2 to 3 ohms-m with temperatures lower than 300 °C. Perhaps a kind of fracturing in a preferential direction is causing an anysotropic effect despite that temperatures are higher or sometimes high temperatures (>200 °C) causes increased resistivity because of less conductive alteration clays. From kilometer 9 to 12, at a depth of 800 m, a resistive is shown, that may correspond again to fresh water intruding from the Colorado river. The later information is supported by agricultural holes beyond the kilometer 12 of this Schlumberger line.
In Figure 4 is shown a resistivity image that was obtained from the inversion of the 20 Schlumberger lines. We only show a horizontal slice at 1300 m depth. Figure 4 shows the main roads, small towns, the railroad, the topographic lines (in meters) of the Cucapá Sierra, the Schlumberger sounding locations and with blue lines, the Colorado and Hardy rivers. In the resistivity image we can see a resistive feature close to the Cucapá Sierra, in the East side there is another resistive zone that corresponds with the spreading of the fresh water of the Colorado river under the surface. The very wide conductor at the south may correspond to salty sediments from the

inundation floods of the Baja California Gulf. The very narrow conductor that separate the two resistive features may correspond with the trace of the Cerro Prieto Fault. There are only surface evidence of this faults close to the center of the image, but to the south it is buried by sediments. The big conductor or set of small conductors at the north of the image are not fully understood, but some small conductors correlate with some surface hydrothermal manifestations. In this image the production zone is colored with green indicating a less conductive behavior than surrounding at 1300 m depth.

5.- CONCLUSIONS

This inversion technique has demonstrated that can be as fast as other new techniques, but also it has the advantage that it does not require to specify an initial model as those using the conventional scattering equations. This technique gives good results in complex geothermal environments. From the resistivity images obtained we can conclude that joint inversion of dipole-dipole and Schlumberger data gives better results than using individual inversion. Despite the general rule, in the Cerro Prieto reservoir it is not always true that higher temperatures correspond to lower resistivities. The horizontal image at a depth of 1300 m shows that most of the important features correspond to the influence of the Cucapá Sierra, the floods of the Baja California Gulf, the fresh water intrusion from Colorado river and perhaps from the Cerro Prieto Fault. We can say very little about the present production zone because there is a lack of resistivity data in such an area.

ACKNOWLEDGEMENTS

We want to thank R. Vázquez, A. Martín, J. Ramírez, J.M. Espinosa, F. Arellano and H. Lira for their comments about the geological and geohydrological background of the geothermal area. Thanks to CFE for allowing us to interpretate the resistivity data, as well as to CICESE and CONACYT for the economical support to do this project. Also thank to H. Benítez for helping us with the drawings.

REFERENCES

Cavazos, R. and Gómez-Treviño, E., 1989, Hacia la inversión tridimensional de anomalias de resistividad y polarización inducida para medios con contraste pequeño en resistividad. *Geofísica Internacional*, Vol. **28** (3), pp. 481-506.

Gómez-Treviño, E., 1987, Nonlinear integral equation for electromagnetic inverse problems. *Geophysics*, Vol. **52**, pp. 1257-1302.

Gupta, V.K and Ramani, N., 1980, Some aspects of regional-residual separation of gravity anomalies in a precambrian terrain, *Geophysics*, Vol. **45** (9), pp. 1412-1426.

Hohmann, G.W., 1975, Three dimensional induced polarization and electromagnetic modeling. *Geophysics*, Vol. **40**, pp. 309-324.

Li, Y. and Oldenburg, D.W., 1992, Approximate inverse mapping in DC resistivity problems. *Geophys. J. Int.,* Vol. **109**, pp. 343-362.

Pérez-Flores, M.A., 1995, Inversión rápida en 2D de datos de resistividad, magnetotelúricos y electromagnéticos de fuente controlada a bajos números de inducción. *Ph.D. Th*esis, CICESE, Ensenada, México.

Pérez-Flores, M.A. and Gómez-Treviño, E., 1997, Dipole-dipole resistivity image of the Ahuachapán-Chipilapa geothermal field, El Salvador. *Geothermics,* Vol. **26** (5/6), pp. 657-680.

Vázquez, R., Ramírez, J., Martín, A., Carreón, C. and García, O., 1998, Estudio geohidrológico del campo geotérmico de Cerro Prieto. *CFE technical report RE-05/98*, Mexican Electrical Comission.

Wilt, M.J., Goldstein, N.E. and Razo, A., 1978. LBL rsistivity studies at Cerro Prieto. First Symposium on the Cerro Prieto Geothermal field.

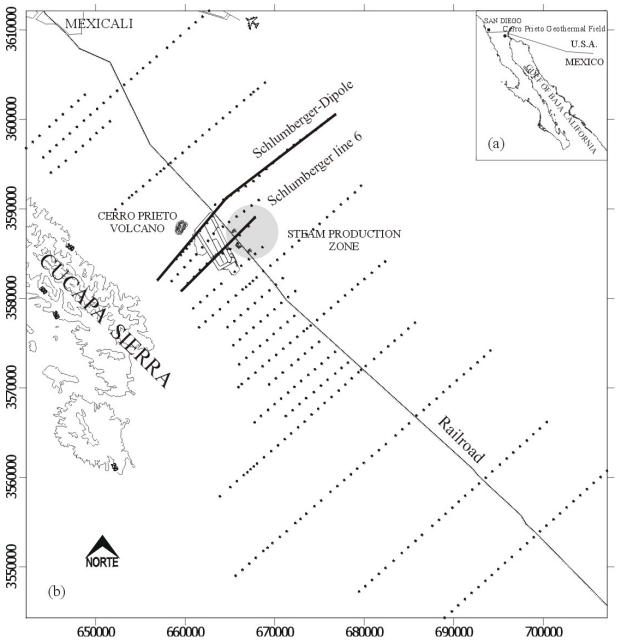

Figure 1.- (a) Location of Cerro Prieto Geothermal area. (b) Distribution of the Dipole-dipole and Schlumberger resistivity lines.

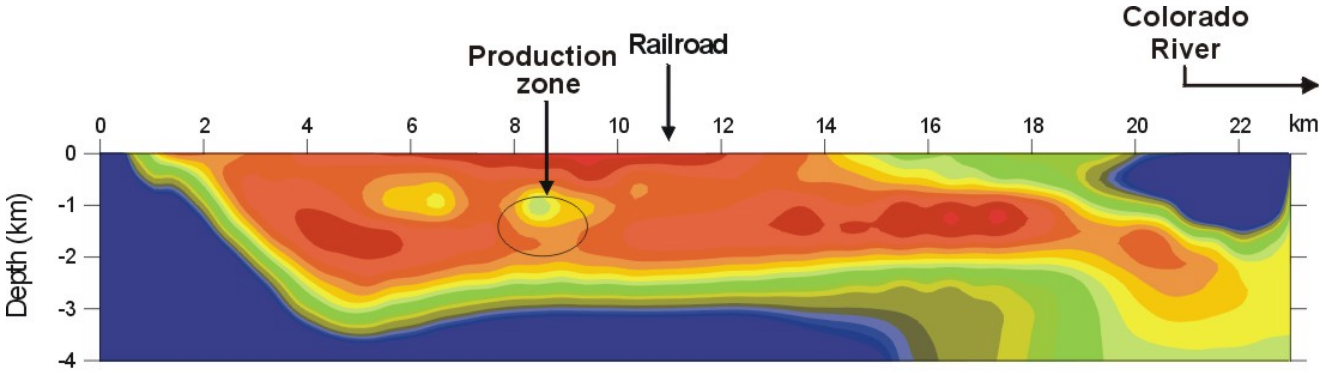

Figure 2.- Joint inversion of Dipole-dipole and Schlumberger resistivity data.

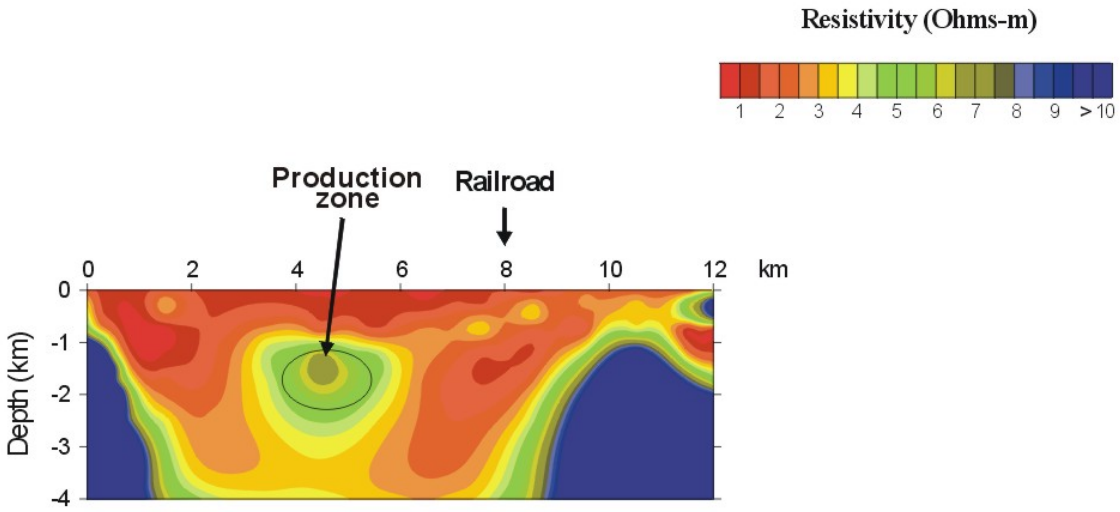

Figure 3.- Resistivity image of the Schlumberger line 6.

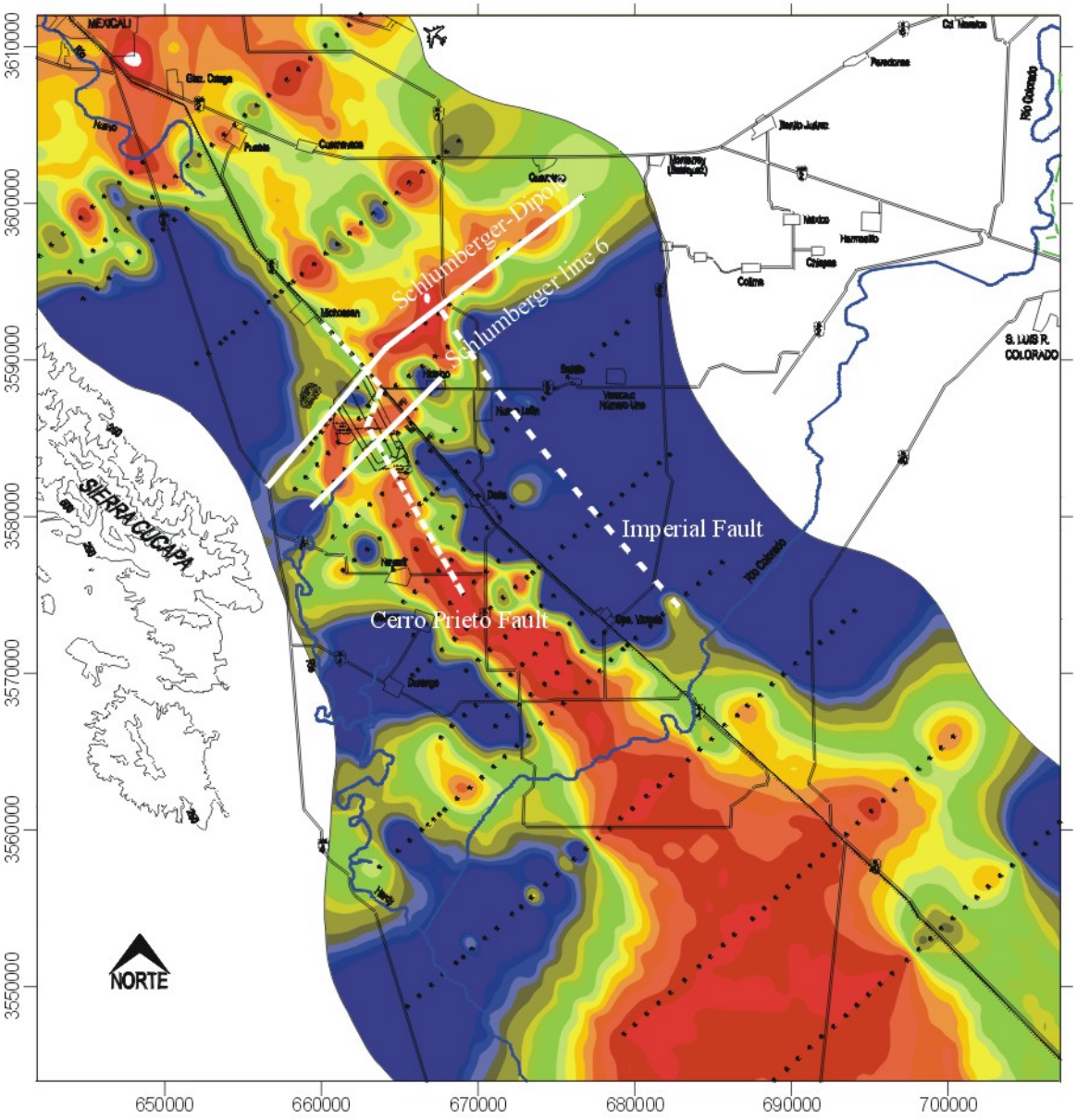

Figure 4.- Resistivity image of the conductive structure on a plane at 1300 m depth.